Noname manuscript No.
(will be inserted by the editor)

J. Math. Biol.
DOI 10.1007/
s00285-010-0328-x

Classical and resource-based competition: A unifying graphical approach

Mary M. Ballyk · Gail S.K. Wolkowicz

Received: date / Accepted: date

Abstract A graphical technique is given for determining the outcome of two species competition for two resources. This method is unifying in the sense that the graphical criterion leading to the various outcomes of competition are consistent across most of the spectrum of resource types (from those that fulfill the same growth needs to those that fulfill different needs) regardless of the classification method used, and the resulting graphs bear a striking resemblance to the well-known phase portraits for two species Lotka-Volterra competition. Our graphical method complements that of Tilman. Both include zero net growth isoclines. However, instead of using the consumption vectors at potential coexistence equilibria

Mary M. Ballyk

Department of Mathematical Sciences, New Mexico State University

MSC 3MB / P.O. Box 30001, Las Cruces, New Mexico, USA 88003-0001

Tel.: (575) 646-6270

Fax: (575) 646-1064

E-mail: mballyk@nmsu.edu

Gail S.K. Wolkowicz

Department of Mathematics and Statistics, McMaster University

1280 Main Street West, Hamilton, Ontario, CANADA L8S 4K1

Tel.: (905) 525-9140 X 24808

Fax: (905) 522-0935

E-mail: wolkowic@mcmaster.ca

to determine input resource concentrations leading to specific competitive outcomes, we introduce curves bounding the feasible set (the set of all potential equilibria). The washout equilibrium (corresponding to the supply point) occurs at an intersection of curves defining the feasible set boundary. The resource concentrations of all other equilibria are found where zero net growth isoclines either intersect each other or the feasible set boundary. A species has positive biomass at such an equilibrium only if its zero net growth isocline is involved in such an intersection. The competitive outcomes are then determined from the position of the single species equilibria, just as in the phase portrait analysis for classical competition (rather than from information at potential coexistence equilibria as in Tilman's method).

Keywords Multiple resource limitation · perfectly substitutable, essential, complementary, homologous, heterologous, interactive, non-interactive · Lotka-Volterra competition · chemostat

Mathematics Subject Classification (2000) MSC 92D25 · MSC 92D40

1 Introduction

We present a graphical method for determining the outcome of two species competition for two resources. This method complements the graphical method of Tilman [25] which is used to determine input resource concentrations leading to specific competitive outcomes. While Tilman's method requires information at potential coexistence equilibria, we introduce curves bounding the feasible set (the set of all potential equilibria). We locate the single species equilibria and coexistence equilibria and then determine the competitive outcomes from the position of the single species equilibria, just as in the phase portrait analysis for classical competition.

The graphical technique illustrated in this paper is presented for the chemostat. However, as in León and Tumpson [17] and Tilman [24], the supply rate of nutrient could be given more generally and species-specific death rates could be introduced. In the present context, our graphical technique is unifying in the following senses. First, the graphical criterion leading to the various outcomes (coexistence, bistability, competitive dominance) are consistent across the spectrum of resource types, regardless of

the classification scheme used. Second, when applied to the classical model of two-species competition (attributed to Lotka [20] and Volterra [27]) where resources are not explicitly modeled, the resulting graph in phase space is startlingly similar to the graphs for the resource based competitive models. This similarity holds despite the fact that the graph is given with respect to population size in the former case and resource concentrations in the latter.

Before considering the resource-based approach, we remind the reader of the classical model and its well-known phase portrait. We then describe our graphical technique. We conclude with a discussion of resource classification issues and a comparison of our graphical method with that of Tilman. Technical details, model derivations, generalizations, and local stability are relegated to appendices.

1.1 Classical Approach

The classical model of ecological competition, attributed to Lotka [20] and Volterra [27], is an extension of the basic logistic model for the growth of a single population due to Verhulst [26], to include interaction terms based on the law of mass action. In the case of n competing populations, for $i = 1, \ldots, n$, the model is given by

$$N_i'(t) = r_i N_i(t) \left(1 - \frac{N_i(t)}{K_i}\right) - \sum_{j=1, j\neq i}^{n} \beta_{ij} N_i(t) N_j(t) \tag{1}$$

For indices $k, \ell \in \{1, 2, \ldots, n\}$, $k \neq \ell$, $N_k(t)$ denotes the size (in density or numbers) of the kth population at time t, r_k denotes the intrinsic growth rate of population k, K_k denotes the carrying capacity of the environment for population k (in the absence of population ℓ), and $\beta_{k\ell}$ denotes the coefficient of competition, measuring the effect of competition on population k due to its interaction with population ℓ.

In the case of two competing species, the dynamics of this system can be determined using a standard phase plane analysis. There are several outcomes possible as depicted in Figure 1: either only one population avoids extinction, or there is coexistence. Complete washout (all solutions tending to $(N_1, N_2) = (0, 0)$) is not possible.

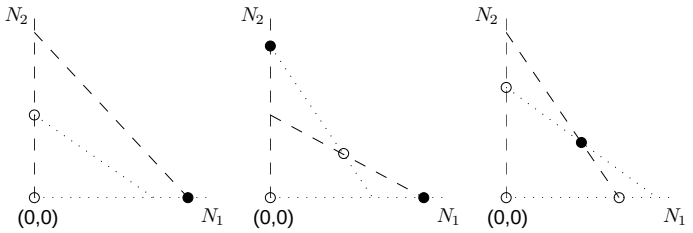

Fig. 1 Potential phase portraits for the classical competition model. Dashed lines are used for the isoclines of population N_1 and dotted lines are used for those of population N_2. Asymptotically stable equilibria are indicated by • and unstable equilibria are indicated by ∘. Dynamics are (LEFT) competitive dominance (i.e., one population wins and drives the other to extinction. In this case population N_1 wins); (CENTRE) initial condition dependent outcome (i.e., the positive equilibrium is a saddle point); (RIGHT) coexistence (i.e., the positive equilibrium is globally asymptotically stable with respect to the positive cone).

1.2 Resource-Based Approach

Consider a general resource-based model describing the competition of n populations, $N(t) = (N_1(t), \ldots, N_n(t))$ for m resources $R(t) = (R_1(t), \ldots, R_m(t))$:

$$\begin{aligned} R_j'(t) &= g_j(R_j(t)) - \sum_{i=1}^{n} N_i(t)\mu_{ij}(R(t)), \\ N_i'(t) &= N_i(t)(-D_i + \mu_i(R(t))), \end{aligned} \tag{2}$$

$$R_j(0),\ N_i(0) \geq 0.$$

Here, $N_i(t),\ i = 1, \ldots, n$ denotes the biomass of the ith population of microorganisms at time t and $R_j(t),\ j = 1, \ldots, m$ represents the concentration of the jth resource at time t.

The functions $g_j(R_j(t))$ denote the supply rate of the resource j. Each D_i can either denote the ith species specific death rate or the sum of a species specific death rate and a dilution rate. For example, Phillips [21] introduced model (2) with $g_j(R_j(t)) = (S_j - R_j(t))D$, as a model of the chemostat, where D denotes the dilution rate and S_j denotes the concentration of resource j in the feed vessel when only one feed vessel is used. (See Butler and Wolkowicz [7] for the interpretation if more than one feed vessel is used.)

The functions $\mu_{ij}(R)$ denote the rate of consumption of resource j by population i per unit of biomass of population i and the functions $\mu_i(R)$ denote the growth rate of population i per unit of biomass of population i. These are given as functions of the concentration of all of the limiting resources in the environment. It is generally assumed that $\mu_i,\ \mu_{ij} : \mathbb{R}_+^m \to \mathbb{R}_+$ and that the μ_i, μ_{ij} are continuously differentiable almost everywhere. Also, it is natural to expect (and we will assume throughout) that if the concentration of resource R_j is zero, there will be no consumption of resource R_j (so that $\mu_{ij}(R) = 0$ whenever $R_j = 0$) and no growth on resource R_j. Note that we make no explicit assumptions regarding the relationship between the functions describing consumption and the functions describing growth, making model (2) very general.

We illustrate the method in the context of two species competing for two resources using the two most familiar resource-based models, one on each end of the resource spectrum. (See the Appendix B for more details concerning the two resource-based models.) As in Phillips [21], we set $g_j(R_j) = (S_j - R_j)D$ in model (2) and make the usual simplifying assumption that the species specific death rates are insignificant compared to the flow rate, i.e., $D_i = D, \quad i = 1, 2.$

In both examples, it is reasonable to assume that the consumption of resource j by population i, $\mu_{ij}(R_1, R_2)$, increases with the availability of that resource. That is,

$$\frac{\partial \mu_{ij}}{\partial R_j}(R_1, R_2) \geq 0, \quad \text{for all} \quad R_1, R_2 > 0, \quad i, j \in \{1, 2\}. \tag{3}$$

In the first example it is assumed that the resources fulfill different growth needs and so must be consumed together in order to promote growth. To derive the model in the form most often considered in the literature [7, 11, 15, 16, 17, 18, 19, 24, 25], the Law of the Minimum is used, giving

$$\begin{aligned} R_j' &= (S_j - R_j)D - \sum_{i=1}^{2} \frac{N_i}{Y_{ij}} \min\{p_{i1}(R_1), p_{i2}(R_2)\}, \\ N_i' &= N_i(-D + \min\{p_{i1}(R_1), p_{i2}(R_2)\}), \end{aligned} \tag{4}$$

$$R_j(0), N_i(0) \geq 0, \quad i, j \in \{1, 2\}.$$

Here, the Y_{ij} denote growth yield constants, and (consistent with (3)) it is assumed that $p_{ij} : \mathbf{R}_+ \to \mathbf{R}_+$ are C^1 with

$$p_{ij}(0) = 0, \quad p'_{ij}(R_j) > 0, \quad \text{for} \quad R_j > 0, \quad i, j \in \{1, 2\}. \tag{5}$$

A prototype is the Michaelis-Menten or Monod functional response to a single resource:

$$p_{ij}(R_j) = \frac{m_{ij} R_j}{K_{ij} + R_j}.$$

However, we will only assume (5), and will even relax this in Appendix C where we consider generalizations. Such resources are referred to as essential by those using the classification of Tilman [24] and perfectly complementary by those using the classification León and Tumpson [17]. In Appendix B.1 we show that to obtain model (4), it seems necessary to assume additionally that consumption of the two resources is in the correct proportions required for growth, thus avoiding any waste.

In the second example, we consider resources that fulfill the same growth needs, i.e., each can sustain growth in the absence of the other. In this case growth is often modeled (e.g. [3, 17, 22]) by a sum of the form:

$$\mu_i(R_1, R_2) = Y_{i1}\mu_{i1}(R_1, R_2) + Y_{i2}\mu_{i2}(R_1, R_2), \tag{6}$$

where the constants Y_{ij} again represent growth yield constants. It might be reasonable to assume that growth by species i increases with resource availability:

$$\frac{\partial \mu_i}{\partial R_j}(R_1, R_2) > 0, \quad \text{for} \quad R_1, R_2 > 0, \quad i, j \in \{1, 2\}. \tag{7}$$

To capture the possible inhibitory effect that the abundance of one resource might have on consumption of the other due to handling time (see [3, 22]), it might be reasonable to assume that while consumption of a resource strictly increases with its availability, so that

$$\frac{\partial \mu_{ij}}{\partial R_j}(R_1, R_2) > 0, \quad \text{for} \quad R_1, R_2 > 0, \quad i, j \in \{1, 2\}, \tag{8}$$

it also decreases with increasing availability of the other resource:

$$\frac{\partial \mu_{ij}}{\partial R_k}(R_1, R_2) \leq 0, \quad \text{for} \quad R_1, R_2 > 0, \quad i, j, k \in \{1, 2\}, j \neq k. \tag{9}$$

For example, the familiar Michaelis-Menten or Monod functional response generalized to the case of two substitutable resources (see [28]) always satisfies (8) and (9). It also satisfies (7) for most reasonable operating parameters. (See [4] for more details.) In this case model (2) becomes:

$$\begin{aligned} R_j' &= (S_j - R_j)D - \sum_{i=1}^{2} \frac{N_i}{Y_{ij}} \left(\frac{m_{ij} K_{ik} R_j}{K_{i1}K_{i2} + K_{i2}R_1 + K_{i1}R_2} \right), \\ N_i' &= N_i \left(-D + \frac{m_{i1}K_{i2}R_1 + m_{i2}K_{i1}R_2}{K_{i1}K_{i2} + K_{i2}R_1 + K_{i1}R_2} \right), \\ & R_j(0), N_i(0) \geq 0, \quad i,j,k \in \{1,2\}, \ k \neq j, \end{aligned} \tag{10}$$

and the resources are considered perfectly substitutable in both the classification of Tilman and of León and Tumpson.

2 Graphical Method

We now describe a graphical method for determining the outcome of competition using the phase plane in (R_1, R_2)-space. The method will be described for the general model (2), and illustrated for models (4) and (10).

To begin we describe the "feasible set" $\mathcal{F}$ in (R_1, R_2)-space, where the (R_1, R_2)-coordinate of any equilibrium must be located. The boundary consists of curves along which $R_1' = 0 = R_2'$, $N_i = 0$, and $N_j \geq 0$, and so passes through the (R_1, R_2)-coordinates of single-species equilibria. The point (S_1, S_2), called the *supply point* in (R_1, R_2)-space, corresponds to the washout equilibrium in (R_1, R_2, N_1, N_2)-space, and is found where the feasible set boundary for the two populations intersect. We then include the zero net growth isoclines, curves in (R_1, R_2)-space along which the populations are neither increasing nor decreasing (found by setting $N_1' = 0 = N_2'$ with $N_1 N_2 \neq 0$). The(R_1, R_2)-coordinates of equilibria are located at the intersections of these curves. A single species equilibrium for a particular population corresponds to where its zero net growth isocline intersects the feasible set boundary corresponding to the absence of the other species. Coexistence equilibria correspond to where the zero net growth isoclines of both species intersect inside the feasible set. Stability of the equilibria is then determined from their location on the graph, analogous to the phase plane analysis for the classical model.

Step 1: Find the Feasible Set Boundary (FSB) for each population and plot them in (R_1, R_2)-space using different line types for each population.

The feasible set boundary for population i (FSB_i) is a curve in (R_1, R_2)-space along which population i is at zero density. To find FSB_i, set $N_i = 0$ in (2) with $g_j(R_j) = (R_j - S_j)D$ and solve $R_1' = 0 = R_2'$ for N_j, so that

$$\frac{(S_1 - R_1)D}{\mu_{j1}(R_1, R_2)} = N_j = \frac{(S_2 - R_2)D}{\mu_{j2}(R_1, R_2)}. \tag{11}$$

Eliminate N_j and plot the resulting curve in (R_1, R_2)-space starting at the supply point and moving toward the axes. On this curve N_i is zero and N_j is positive (except at the supply point).

For model (4) this gives

$$R_2 = S_2 - \frac{Y_{j1}}{Y_{j2}}(S_1 - R_1), \tag{12}$$

a line joining the supply point to the coordinate axes (see Figure 2 (TOP)).

For model (10) this gives

$$R_2 = \frac{K_{j2} m_{j1} S_2 R_1}{K_{j1} m_{j2}(S_1 - R_1) + K_{j2} m_{j1} R_1},$$

a curve joining the supply point to the origin (see Figure 2 (BOTTOM)).

Step 2: Identify the Feasible Set $\mathcal{F}$ (where the (R_1, R_2)-components of any equilibrium must be located) as the bounded region with boundary defined by the portion of each FSB from the supply point to its intersection with a coordinate axis as well as (by continuity) the portion of the coordinate axes between these intersections.

Typical feasible sets are depicted by the shaded regions in Figure 2 (TOP) for model (4) and (BOTTOM) for model (10). For convenience, we use the leftmost configurations in what follows.

Step 3: Find the Zero Net Growth Isocline (ZNGI) for each population and plot them in (R_1, R_2)-space using the same line type used for population i as used for its FSB_i.

The ZNGI for population i (ZNGI_i) is the curve of resource concentrations along which the decline in biomass density is balanced by its growth and so the net biomass of that population remains unchanged.

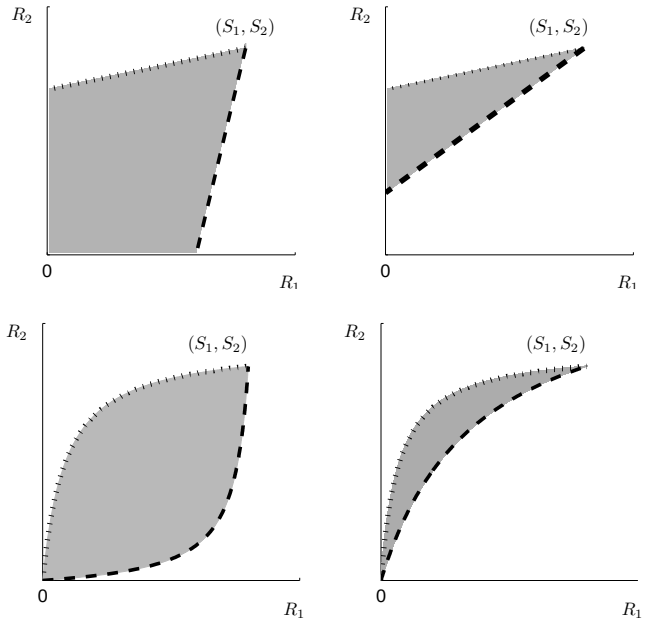

Fig. 2 The dashed and dotted curves correspond to FSB_1 and FSB_2, respectively. The shaded regions indicate typical feasible sets in the case of (TOP) model (4) and (BOTTOM) model (10). The biomass at potential equilibria of both populations is nonnegative for resource concentrations inside the feasible set, and at least one population would have negative biomass outside.

To determine the zero net growth isocline for population i (ZNGI_i), set $N_i' = 0$ with $N_i \neq 0$, so that

$$\mu_i(R_1, R_2) = D. \tag{13}$$

For model (4) the ZNGI_i correspond to L-shaped curves in (R_1, R_2)-space with vertex at (R_{1_i}, R_{2_i}) (see Figure 3 (TOP)) and for model (10) to a line in the (R_1, R_2)-plane joining $(R_{1_i}, 0)$ to $(0, R_{2_i})$ (see Figure 3 (BOTTOM)). See Appendix A for the definition of the generalized break-even concentrations R_{j_i}, in each case.

Step 4: Define the Invasive Set $\mathcal{I}_i$ as those resource concentrations in the feasible set that are sufficient so that the decline of population i is at least balanced by its growth. Therefore, if ZNGI_i intersects the feasible set $\mathcal{F}$, it divides $\mathcal{F}$ into two regions,

$$\mathcal{I}_i = \{(R_1, R_2) \in \mathcal{F} : \mu_i(R_1, R_2) \geq D\},$$

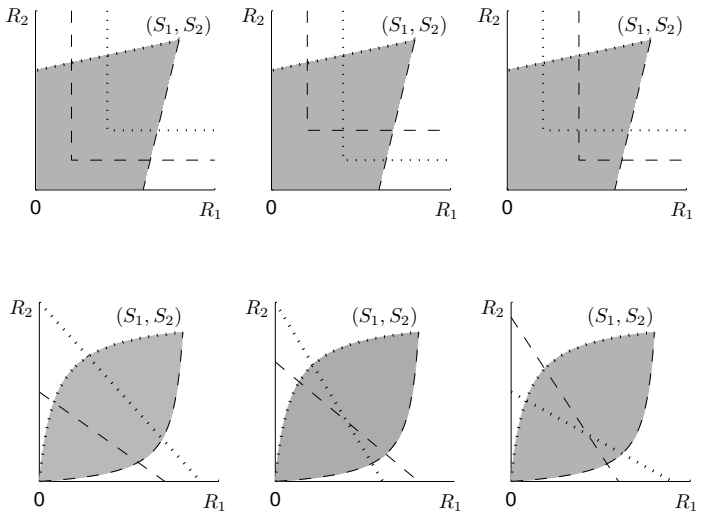

Fig. 3 The ZNGIs are included with the feasible sets in the case of (TOP) model (4) and (BOTTOM) model (10). ZNGI_1 and FSB_1 are dashed; ZNGI_2 and FSB_2 are dotted. The invasive set $\mathcal{I}_i$ corresponds to that portion of the feasible set $\mathcal{F}$ (shaded region) between the supply point and ZNGI_i, i.e. the portion of $\mathcal{F}$ above and to the right of ZNGI_i.

and its complement. (See Figure 3.) Observe that since the resources are noninhibitory, $(S_1, S_2) \in \mathcal{I}_i$.

We call $\mathcal{I}_i$ the invasive set for species i, since we will show that if the single species equilbrium for species j (i.e. with $N_j > 0$) lies inside $\mathcal{I}_i$, then species i can invade (and hence that single species equilibrium is unstable). However, if the single species equilbrium for species j lies outside $\mathcal{I}_i$, then species i cannot invade (and the equilibrium is locally asymptotically stable).

Step 5: Identify Equilibria

Each intersection of a dashed curve and a dotted curve in the feasible set corresponds to an equilibrium point (except at the origin). N_i is positive at such an equilibrium point, if and only if ZNGI_i is involved in the intersection.

- The intersection of the two FSBs at the supply point corresponds to the washout equilibrium.
- Any point where a population's ZNGI_i intersects an FSB_j (with $i \neq j$), corresponds to a single species equilibrium with that population present, i.e. $N_i > 0$.

– Points where ZNGI_1 and ZNGI_2 intersect in the interior of $\mathcal{F}$ correspond to coexistence equilibria, i.e. both species present.

Step 6: Determine the Stability of Equilibria and the Outcome of Competition

We begin by assuming that ZNGI_i intersects both FSB_j and ZNGI_j at most once, $i, j \in \{1, 2\}$, $i \neq j$, and that at any such intersection the curves actually cross (i.e. the intersection is transversal). In Appendix C we examine the implications of generalizing to multiple crossings of ZNGI_i and FSB_j (C.1) and multiple crossings of the ZNGI (C.2).

Any intersection of a ZNGI_i with an FSB_j represents a single species equilibrium with N_i positive. We also assume that this equilibrium would be globally asymptotically stable in the corresponding growth model, i.e., with respect to the (R_1, R_2, N_i)-subsystem. These assumptions hold, for example, for models (4) and (10), for the classical two species Lotka-Volterra competition model (1) if viewed in this context (as will be described in Section 3), and even more generally (see Appendix C.3).

– If neither ZNGI intersects $\mathcal{F}$, the invasive set for both species is empty and so neither species can invade. In this case the washout equilibrium is globally asymptotically stable. Otherwise, the invasive set of at least one species is non-empty and contains the supply point. At least one species can invade and so the washout equilibrium is unstable. The former is depicted in Figure 4 (TOP) for both model (4) (LEFT) and model (10) (RIGHT).

– If only ZNGI_i intersects FSB_j, $i \neq j$, then there is a unique single species equilibrium where population N_i is positive. The invasive set $\mathcal{I}_i$ contains the supply point so that species i can invade and the washout equilibrium is unstable. However, $\mathcal{I}_j = \emptyset$, so species j cannot invade and the single species equilibrium (involving N_i) remains locally asymptotically stable, now with respect to (R_1, R_2, N_1, N_2)-space. Species i is the only survivor. This is depicted in Figure 4 (BOTTOM) for both model (4) (LEFT) and model (10) (RIGHT) .

– If each ZNGI_i intersects FSB_j, $(i, j = \{1, 2\},\ i \neq j)$, then there are two single species equilibria, one for each population. Population N_i is positive where ZNGI_i is involved in the intersection. If population N_i's single species equilibrium lies in $\mathcal{I}_j$, then population j can invade, and hence popu-

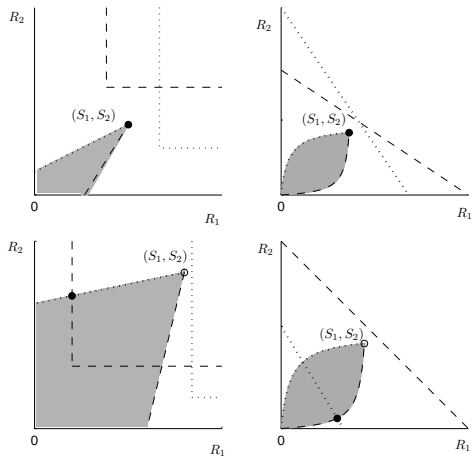

Fig. 4 Potential phase portraits for (LEFT) model (4); (RIGHT) model (10). Asymptotically stable equilibria are indicated by • and unstable equilibria are indicated by ∘. (TOP) When neither ZNGI intersects the feasible region, the washout equilibrium is globally asymptotically stable: (BOTTOM) If one and only one of the ZNGI intersects $\mathcal{F}$, then there is a unique single species equilibrium that is locally asymptotically stable: (LEFT) with population N_1 (dashed) positive, since ZNGI_1 is involved in the intersection; and (RIGHT) with population N_2 (dotted) positive, since ZNGI_2 is involved in the intersection.

lation N_i's single species equilibrium is unstable with respect to (R_1, R_2, N_1, N_2)-space. Otherwise, it remains locally asymptotically stable.

- When both single species equilibria are of opposite stability, the unstable one lies inside the invasive set of its competitor and the stable one lies outside the invasive set of its competitor. Since the ZNGI intersect at most once, there is no coexistence equilibrium and we have competitive dominance. This is shown in Figure 5 (LEFT) for both model (4) (TOP) and model (10) (BOTTOM).
- When the single-species equilibria have the same stability, each either lies inside the invasive set of its competitor (so that both are unstable), or lies outside the invasive set of its competitor (so that both are locally asymptotically stable).
- If both single-species equilibria are stable, then the ZNGIs intersect at a unique coexistence equilibrium in $\mathcal{F}$ and it is unstable. This corresponds to initial condition dependent outcomes, and is illustrated in Figure 5 (CENTER) for both model (4) (TOP) and model (10) (BOTTOM). See Appendix D.2 for justification of the instability of the coexistence equilibrium.

– If both single species equilibria are unstable, then the ZNGIs intersect at a unique coexistence equilibrium in $\mathcal{F}$ and it is stable up to Hopf bifurcation. This is illustrated in Figure 5 (RIGHT) for both model (4) (TOP) and model (10) (BOTTOM). (Again, see Appendix D.2 for a discussion of the stability of the coexistence equilibrium.) However, it can be shown that the system is uniformly persistent whether or not there is a Hopf bifurcation, so that both species coexist. The proof of this involves an argument similar to the proof given for Theorem 3.16 in [3] using the Butler-McGehee Lemma (see Lemma A.1 of [9]).

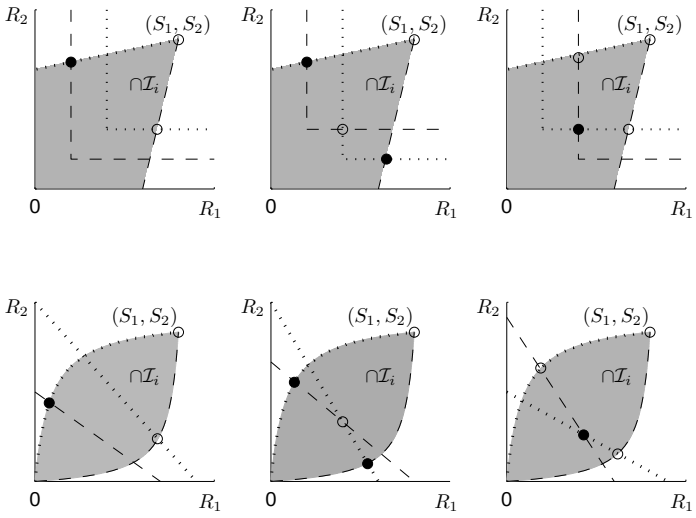

Fig. 5 Potential phase portraits for (TOP) model (4) and (BOTTOM) model (10). Dynamics are (LEFT) competitive dominance (N_1 (dashed) wins and drives N_2 (dotted) to extinction); (CENTRE) initial condition dependent outcome (the positive equilibrium is a saddle point); (RIGHT) coexistence (either the positive equilibrium is locally asymptotically stable or it has undergone a Hopf bifurcation). Here again asymptotically stable equilibria are indicated by • and unstable equilibria are indicated by ∘, except in (RIGHT), where • in the interior of the feasible region indicates uniform persistence. Note that $\cap\mathcal{I}_i$ corresponds to that portion of the shaded region above and to the right of both ZNGIs.

3 Graphical method applied to classical model (1)

The graphical method presented in Section 2 is basically a generalization of the standard phase plane analysis for the classical two species Lotka-Volterra competition model if one notes that the equilibria of the resource-based model actually have four components, and so are of the form $(\bar{R}_1, \bar{R}_2, \bar{N}_1, \bar{N}_2)$. Therefore, points in (R_1, R_2)-space correspond naturally to points in (N_1, N_2)-space. For example, the supply point (S_1, S_2) corresponds to the washout equilibrium $E_0 = (S_1, S_2, 0, 0)$ and hence to the origin in (N_1, N_2)-space. All other equilibria correspond to points in (N_1, N_2)-space with either only one component positive (single species equilibria) or with both components positive (coexistence equilibria). As well, the feasible set boundaries correspond to the coordinate axes, the feasible set to the entire first quadrant, and ZNGIs to the usual isoclines joining the axes:

$$N_i + \frac{\beta_{ij} K_i}{r_i} N_j = K_i, \ i, j \in \{1, 2\}, \ i \neq j.$$

The invasive set is that part of the feasible set on the side of the isocline containing the origin:

$$\mathcal{I}_i = \{(N_1, N_2) \in \mathcal{F} : N_i + \frac{\beta_{ij} K_i}{r_i} N_j \leq K_i\}, \ i, j \in \{1, 2\}, \ i \neq j.$$

In the classical model it is understood that the carrying capacity of each population is positive, and hence the ZNGI of each population intersects the feasible set. The identification of equilibria works exactly the same as in Step 5 of Section 2. The determination of the stability of equilibria and the outcome of competition follows just as it does in Step 6 of Section 2 (see Figure 6). Observe that the washout equilibrium is always in the invasive set of both species and so is always unstable.

4 Discussion

4.1 Classification Issues

In this paper we consider multiple resource competition in the chemostat for fixed input resource concentrations. We begin by describing a general mathematical model in system (2). When more than one

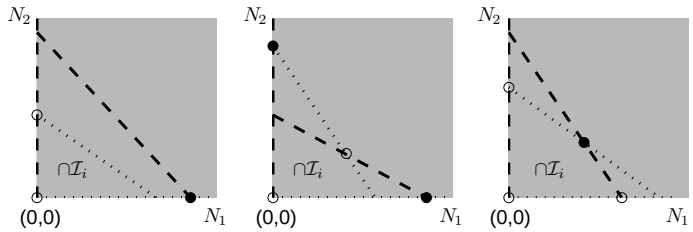

Fig. 6 Potential phase portraits for the classical competition model. Dynamics are (LEFT) competitive dominance; (CENTRE) initial condition dependent outcome; (RIGHT) coexistence. The invasive set $\mathcal{I}_i$ for each species corresponds to that portion of the feasible set $\mathcal{F}$ (shaded region) between the origin (identified with the supply point) and ZNGI_i. Therefore, $\cap\mathcal{I}_i$ corresponds to that portion of the shaded region below and to the left of both ZNGIs.

resource is potentially limiting, it becomes important to consider how resources are consumed and then used by the competitors. Several authors have considered this issue and different terminology has been proposed (e.g., [1, 2, 8, 17, 23, 24, 25]) to classify the spectrum of resource types: from resources that fulfill different growth needs on the one extreme to resources that fulfill the same growth needs on the other extreme.

With multiple limiting resources, it is necessary to consider how consumption and growth are affected by changes in resource concentration. León and Tumpson [17] and Rapport [23] classify resources in terms of how they fulfill nutritional requirements, and obtain a spectrum of resource types: perfectly substitutable resources, imperfectly substitutable resources, and perfectly complementary resources. The tool they use to classify resource pairs is *indifference curves*. Here, the curve $\mu_i(\mu_{i1}, \mu_{i2}) = C$ projected onto the (μ_{i1}, μ_{i2})-plane give pairs of values of μ_{i1} and μ_{i2} for which the growth rate is constant. They call resources for which indifference curves are linear perfectly substitutable resources. Such resources are alternative sources of the same required nutrient. An example for a bacterium might be two carbon sources or two sources of nitrogen. Related studies include [5, 3, 22, 28]. At the other extreme are the perfectly complementary resources (for which indifference curves form rectangular corners). These fulfill different growth needs, and so must both be consumed in order to promote growth. For example, a nitrogen source and a carbon source might be classified as essential for a bacterium. Related studies include [7, 15, 16, 17, 19, 23, 28]. Nutrients that fall into neither of these categories fill out the spectrum

and are referred to as imperfectly substitutable. The species could survive on either of these resources alone, but growth is enhanced when the resources are combined. In this case, the indifference curves are convex to the origin.

Tilman [24] classifies resources according to the shape of the *resource growth isoclines*, i.e. the shape of the curves $\mu_i(R_1, R_2) = C$ projected onto the (R_1, R_2)-plane instead of the (μ_{i1}, μ_{i2})-plane. (See Figure 2 of [24].) Resources are substitutable when one can sustain the population in the absence of the other. For such resources, the resource growth isoclines intersect the R_1 and R_2 axes. These range from complementary (bowing toward the origin) through perfectly substitutable (straight lines) and antagonistic (bowing away from the origin) to switching (forming right angle corners pointing away from the origin). When one resource is required and the other may partially substitute for the first, the resources are termed hemi-essential; here, the resource growth isoclines cross one of the resource axes but eventually run parallel to the other. Resources are essential with respect to each other when both are required for growth. The resource growth isoclines for *perfectly* essential resources form right-angled corners pointing toward the origin. In some cases such resources are also perfectly complementary in the sense of León and Tumpson [17]. Hence there are two potential sources of confusion: the use of the same terms for different resource types and the use of different terms for the same resource types. For interactive essential resources, the corner is replaced by a curve. Finally, resources that inhibit growth at high concentrations will yield resource growth isoclines that form closed curves. Other terminology introduced to describe mixed substrate utilization for nutrients that satisfy the same physiological requirements for growth include homologous (Harder and Dijkhuizen [12]) or non-interactive (Bader et al [2]), whereas heterologous (Egli [8]) and interactive (Bader [1]) have been used for nutrients that satisfy different physiological requirements. The graphical method presented here does not depend on the terminology chosen to classify resources. Though it involves the curve $\mu_i(R_1, R_2) = C$, it is of no consequence whether this curve represents a resource growth isocline or is obtained by projecting an indifference curve into the (R_1, R_2)-plane.

It has been well-established [6, 13, 14, 29] that the basic model of exploitative competition in the chemostat for a single, non-reproducing, growth-limiting resource predicts that at most one population will survive. This remains the case when the model is refined to include a delay in the process of conversion of nutrient to viable biomass (see e.g., [30, 31, 32]), and is in keeping with the principle of competitive exclusion: two populations that compete for the exact same resources cannot stably coexist [10]. We restrict our attention to two populations competing for two resources, in order to compare the possible outcomes of the classical model (where coexistence is possible) with those of the resource-based approach. We find that the general framework provided by system (2) is adequate to capture virtually all of the resource types described in this section. The details of the corresponding model derivations for the extremes is provided in Appendix B.

4.2 Unification with classical model and across resource types

Given that system (2) is four-dimensional, it might be surprising that the graphical method of Section 2 allows for meaningful graphical comparisons with the two-dimensional classical model (1). The remarkable correspondence between the phase portraits is depicted in Figure 7. In these figures, dashed lines are used for the isoclines of species N_1 and dotted lines are used for those of species N_2. Recall that the supply point (S_1, S_2) in (R_1, R_2)-space corresponds to the extinction equilibrium point $(0, 0)$ in (N_1, N_2)-space. Since the phase portraits for model (4) and model (10) are shown in (R_1, R_2)-space, the phase portraits in the classical case (Figure 6) are shown upside down in (N_1, N_2)-space in order to emphasize the similarity.

In the leftmost column, the outcome of competition for each system is competitive dominance, i.e. species N_1 wins and drives species N_2 to extinction. In each case the ZNGIs do not intersect inside the feasible region, so that there is no coexistence equilibrium. The single species equilibrium where N_2 is positive lies in $\mathcal{I}_1$, so that species 1 can invade and the equilibrium is unstable. At the same time, the

single species equilibrium where N_1 is positive is not in $\mathcal{I}_2$, so that species 2 cannot invade and the equilibrium is stable.

In the center column, the outcome of competition for each system is initial condition dependent (i.e., the positive equilibrium is unstable and there are two stable single species equilibria). In each case the ZNGIs intersect inside the feasible region, so that there is a coexistence equilibrium. Each single species equilibrium lies outside the invasive set of the other species, and hence is stable. Since both single species equilibria are stable, the coexistence equilibrium is unstable (see Step 6 of Section 2).

In the rightmost column, competition results in the survival of both species. In each case the ZNGIs again intersect inside the feasible region, so that there is a coexistence equilibrium. Here, each single species equilibrium lies inside the invasive set of the other species, and hence is unstable. Since both single species equilibria are unstable, the coexistence equilibrium is stable (up to Hopf bifurcation), and the system is uniformly persistent. For related global results, see [3, 6].

Notice that the figures in each column are topologically equivalent in the sense that if one stretches the zero net growth isoclines in the second row so that they are all straight lines, then the graph would look the same as the graph in the bottom row. Figure 7$_{(\text{MIDDLE})}$ (where resources fulfill different needs) and Figure 7$_{(\text{BOTTOM})}$ (where resources fulfill the same needs) represent extremes in a continuum of resource types. Typical resources likely fall between these extremes. The continuous deformation of one set of figures to the other will preserve the basic structure, thus demonstrating a unification across resource types. Moreover, the dynamics in any given column is consistent, thus demonstrating a unification of the resource-based models with the classical model in the context of the graphical method described herein.

4.3 Comparison with Tilman's Graphical Method

In a series of papers and monographs [24, 25], Tilman examines two-species competition for two resources. There it is assumed that growth rate depends directly on resource availability and that the consumption rate has the special form $\mu_{ij}(R) = \mu_i(R)h_{ij}(R)$, where $h_{ij}(R)$ is the function describing the amount of

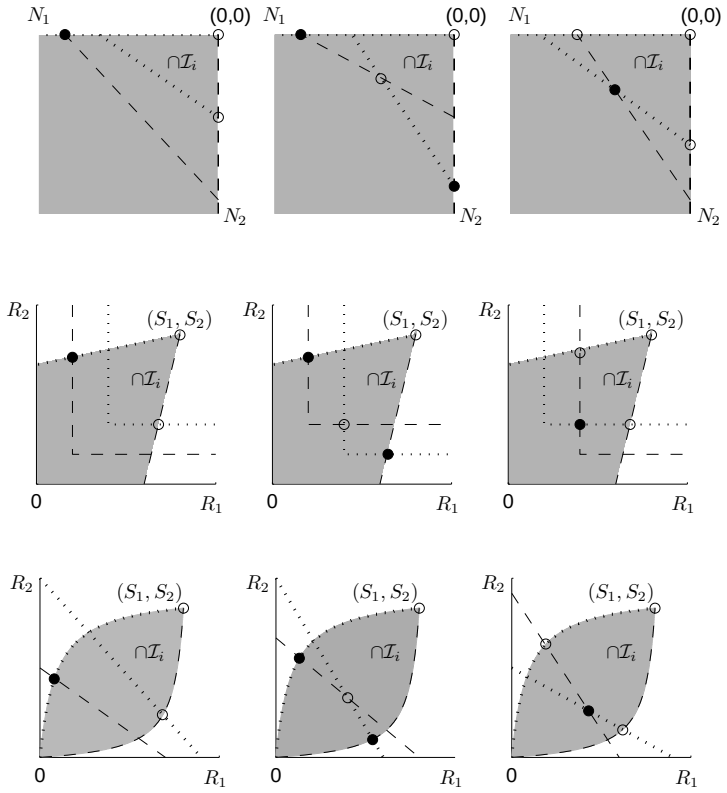

Fig. 7 Similarity of the phase portraits in the case of: (TOP) classical; (MIDDLE) model (4); (BOTTOM) model (10). Dashed lines are used for species N_1 and dotted lines for species N_2. The symbols • and ∘ are as in Figure 5. The phase portraits in the classical case are shown upside down in (N_1, N_2)-space, in order to emphasize the similarity. Dynamics are (LEFT) competitive dominance (species N_1 wins and drives species N_2 to extinction); (CENTRE) initial condition dependent outcome; (RIGHT) coexistence. Notice that if one identifies $(0, 0)$ with (S_1, S_2) and stretches the figures in the second and third rows so that the isoclines are all straight lines, then they would look essentially the same as the figure for the classical case just above them.

resource R_j required to produce each new individual of species N_i. We feel it is reasonable to assume that the functions describing the rate of consumption of resources, μ_{ij}, should depend directly on resource availability. Although not necessary for our analysis, we think that the functions modelling the growth rate, μ_i, on the other hand, should be a function of the amount of each resource consumed, and hence depend only indirectly on the availability of the resources, as given by

$$\mu_i(R(t)) = \mu_i(\mu_{i1}(R(t)), \mu_{i2}(R(t)), \ldots, \mu_{im}(R(t))).$$

With the notable exception of essential, switching, and inhibitory resources, all of the resource types described by Tilman produce resource growth isoclines (and hence ZNGIs) corresponding to decreasing functions in the (R_1, R_2)-plane. If one imposes only condition (7) on model (2), only monotone decreasing ZNGIs are obtained. With the addition of ((8) and (9)) or ((8) and (21)), FSB_j is monotone increasing (Appendix C.1) so that ZNGI_i and FSB_j can intersect at most once, and at most one single-species equilibrium can exist. Moreover, a single-species equilibrium is locally asymptotically stable in the corresponding three-dimensional subsystem when it exists (see [21]). The local asymptotic stability of single-species equilibria in the full four-dimensional system then follow from the invasion criterion, as described in Section 4.2.

In the context of model (2), Tilman would define the consumption vector of species i at resource concentration (R_1^*, R_2^*) to be

$$\mathbf{c_i} = \begin{pmatrix} \mu_{i1}(R_1^*, R_2^*) \\ \\ \mu_{i2}(R_1^*, R_2^*) \end{pmatrix}.$$

He further determines ZNGIs precisely as in Step 3. Tilman divides (R_1, R_2)-space into regions based on the relative positions of the ZNGIs and the slopes of the consumption vectors at the intersection of the ZNGIs (if any). Different competitive outcomes can be obtained depending on the region in which (S_1, S_2) is located. (See Figure 24 of [25].)

When the ZNGIs do not intersect (see Figure 5 (LEFT)), the pattern of dominance (as a function of the location of the supply point) is easily supported by our graphical technique. When the two ZNGIs intersect (see Figure 5 (CENTER) and (RIGHT)), Tilman considers the system of equations obtained by setting $R_1' = 0 = R_2'$. (These equations, together with the condition $N_i = 0$, were used in Step 1 to determine FSB_i.) At the intersection (R_1^*, R_2^*) of the ZNGIs, this yields

$$\begin{aligned} \sum_{i=1}^{2} N_i \mu_{i1}(R_1^*, R_2^*) &= (S_1 - R_1^*)D, \\ \\ \sum_{i=1}^{2} N_i \mu_{i2}(R_1^*, R_2^*) &= (S_2 - R_2^*)D. \end{aligned} \tag{14}$$

He considers this to be a linear system for N_1^* and N_2^*, and solves to obtain

$$N_1^* = \frac{(S_1 - R_1^*)\mu_{22}(R_1^*, R_2^*) - (S_2 - R_2^*)\mu_{21}(R_1^*, R_2^*)}{\Delta(R_1^*, R_2^*)},$$
$$N_2^* = \frac{(S_2 - R_2^*)\mu_{11}(R_1^*, R_2^*) - (S_1 - R_1^*)\mu_{12}(R_1^*, R_2^*)}{\Delta(R_1^*, R_2^*)}, \tag{15}$$

where $\Delta(R_1^*, R_2^*)$ is the determinant of the coefficient matrix associated with (14):

$$\Delta(R_1^*, R_2^*) = \mu_{11}(R_1^*, R_2^*)\mu_{22}(R_1^*, R_2^*) - \mu_{12}(R_1^*, R_2^*)\mu_{21}(R_1^*, R_2^*). \tag{16}$$

Let $\mathcal{C}_i$ denote the slope of the consumption vector of species i at the intersection:

$$\mathcal{C}_i = \frac{\mu_{i2}(R_1^*, R_2^*)}{\mu_{i1}(R_1^*, R_2^*)}.$$

Without loss of generality, assume $\mathcal{C}_1 < \mathcal{C}_2$. Noting that each of N_1^* and N_2^* in (15) shares a factor of $\Delta(R_1^*, R_2^*)$, it follows from their numerators that the corresponding solution (N_1^*, N_2^*) will have both coordinates positive provided

$$\mathcal{C}_1 < \frac{(S_2 - R_2^*)D}{(S_1 - R_1^*)D} < \mathcal{C}_2.$$

The left inequality indicates that N_2^* will be positive provided the ratio of the net supply rate of resource two to that of resource one exceeds $\mathcal{C}_1$. Similarly, the right inequality indicates that N_1^* will be positive provided $\mathcal{C}_2$ exceeds the net supply rate of resource two to that of resource one. These inequalities then yield conditions that must be satisfied by the supply point in order to ensure the feasibility of the coordinates of (N_1^*, N_2^*). In particular, the ordered pair (S_1, S_2) must satisfy $R_2^* + DC_1(S_1 - R_1^*) < S_2$ in order to ensure that $N_2^* > 0$ and $S_2 < R_2^* + DC_2(S_1 - R_1^*)$ in order to ensure that $N_1^* > 0$.

In Tilman's graphical method the dilution rate is fixed, and the input nutrient concentrations (S_1, S_2) that lead to specific competitive outcomes are determined based on information at potential coexistence equilibria. That is, determination of the feasibility of (N_1^*, N_2^*) relies on information obtained at the intersection of the ZNGIs. This is in contrast to the graphical method presented here, where existence, location, and stability of single-species equilibria is determined for fixed (S_1, S_2) from single-species

information. For given species and input concentrations, the feasible set is fixed. The zero net growth isoclines (and hence the location of equilibria) move in response to changes in the dilution rate D. Thus, one can progress from Figure 4(TOP) through Figure 4(BOTTOM) to Figure 5 (and hence from washout through competitive exclusion to coexistence) by decreasing D.

Appendices

A ZNGIs and Generalized Break-Even Concentrations

It is well-known that the outcome of competition for a single non-reproducing resource in the chemostat depends on the relative value of the so-called break-even concentrations. In the case of multiple limiting resources there is a surface of break-even concentrations, those values of the vector $R = (R_1, \ldots, R_m)$ such that $\mu_i(R) = D$. In the case of two limiting resources this defines a level curve in (R_1, R_2)-space, typically referred to as a zero net growth isocline, since $N_i' = 0$ at all points on the curve. The nature of this curve will be determined by the manner in which the resources are combined to promote growth.

A.1 Generalized Break-Even Concentrations: Resources fulfill different growth needs as in (4).

In order to describe the zero net growth isoclines for resources fulfilling different growth needs, it will be convenient to establish the following notation for the break-even concentration for population i on resource R_j when the other resource is abundant and hence nonlimiting. Define R_{j_i} so that

$$p_{ij}(R_{j_i}) = D. \tag{17}$$

By the monotonicity of $p_{ij}(R_j)$, R_{j_i} is a uniquely defined extended positive real number provided we assume that $R_{j_i} = \infty$ if $p_{ij}(R_j) < D$ for all $R_j \geq 0$. When both resources are supplied in growth-limiting amounts, we have $\mu_i(R_{1_i}, R_2) = D$ for all $R_2 \geq R_{2_i}$ and $\mu_i(R_1, R_{2_i}) = D$ for all $R_1 \geq R_{1_i}$, giving an L-shaped curve of break-even concentrations with corner at (R_{1_i}, R_{2_i}) in the (R_1, R_2)-plane. More generally, when two resources fulfill different needs (and hence neither can sustain the population independently) the zero net growth isocline need not form corners. However, it does not intersect the R_1 and R_2 axes, but runs parallel to them asymptotically.

A.2 Generalized Break-Even Concentrations: Resources fulfill the same growth needs as in (10).

In order to describe the zero net growth isoclines for resources that fulfill the same growth needs, it will be convenient to establish the following notation for the break-even concentration for population i on resource R_j when the other resource is absent. Since each resource can sustain growth in the absence of the other, there is a finite concentration R_{1_i} of resource R_1 satisfying $\mu_i(R_{1_i}, 0) = D$ and a finite concentration R_{2_i} of resource R_2 with $\mu_i(0, R_{2_i}) = D$. In fact, there is a continuous decreasing function $R_1 = \varphi_i(R_2)$ from $(R_{1_i}, 0)$ to $(0, R_{2_i})$ such that $\varphi_i(0) = R_{1_i}$, $\varphi_i(R_{2_i}) = 0$, and $\mu_i(\varphi_i(R_2), R_2) = D$.

B Model Derivations

B.1 Resources that fulfill different growth needs

We first consider resources that fulfill different growth needs, and so must be used together by the consumer. In this case, the Law of the Minimum is customarily used to model the growth rate based on consumption, giving

$$\mu_i(R_1, R_2) = \min\{Y_{i1}\mu_{i1}(R_1, R_2), Y_{i2}\mu_{i2}(R_1, R_2)\}.$$

Here $Y_{ij} = \frac{1}{c_{ij}}$ is a growth yield factor and c_{ij} denotes the number of units of resource j that an individual of population i must consume in order to produce a new unit of its own biomass. Then model (2) becomes

$$\begin{aligned} R_j' &= (S_j - R_j)D - \sum_{i=1}^{2} N_i \mu_{ij}(R_1, R_2), \\ N_i' &= N_i(-D + \min\{Y_{i1}\mu_{i1}(R_1, R_2), Y_{i2}\mu_{i2}(R_1, R_2)\}), \end{aligned} \tag{18}$$

$$R_1(0),\ R_2(0),\ N_1(0),\ N_2(0) \geq 0.$$

It is reasonable to assume that the consumption of resource j by population i, $\mu_{ij}(R_1, R_2)$, is a monotone increasing function of resource j, as in (3).

To derive the model in the form most often considered in the literature [7, 11, 15, 16, 17, 18, 19, 24, 25], it seems necessary to assume further that consumption of the two resources is also in the correct proportions required for growth, thus avoiding any waste. Hence, the consumption of a resource in abundant supply is dictated by the availability of the other resource when the latter is in relatively short supply. In particular, this means that if $\mu_{i1}(R_1)$ denotes the amount of R_1 that would be consumed by N_i if R_2 is plentiful, then to avoid waste, the corresponding amount of R_2 consumed would have to be $\frac{c_{12}}{c_{11}}\mu_{i1}(R_1)$. Similarly, if $\mu_{i2}(R_2)$ denotes the amount of R_2 that would be consumed by N_i if R_1 is plentiful, then to avoid waste, the corresponding amount of R_1

consumed would have to be $\frac{c_{11}}{c_{12}}\mu_{i2}(R_2)$. Therefore,

$$\mu_{i1}(R_1,R_2)=\min\left\{\mu_{i1}(R_1),\frac{c_{11}}{c_{12}}\mu_{i2}(R_2)\right\}=c_{11}\min\left\{\frac{\mu_{i1}(R_1)}{c_{11}},\frac{\mu_{i2}(R_2)}{c_{i2}}\right\}$$

and

$$\mu_{i2}(R_1,R_2)=\min\left\{\frac{c_{12}}{c_{11}}\mu_{i1}(R_1),\mu_{i2}(R_2)\right\}=c_{12}\min\left\{\frac{\mu_{i1}(R_1)}{c_{11}},\frac{\mu_{i2}(R_2)}{c_{i2}}\right\}.$$

To simplify notation, and have the model appear in the form most familiar in the literature (e.g. [7, 15, 17, 19]), define $p_{ij}(R_j)=\frac{\mu_{ij}(R_j)}{c_{ij}}$ and impose assumption (5) in keeping with (3) to obtain system (4).

The assumption that resources are consumed in the proportions required for growth has lead to one of the most familiar models for multiple resource limitation in the literature, and so this will be one of the models we use to illustrate our graphical method. Since the indifference curves (in the (μ_{i1},μ_{i2})-plane) for this model are right-angled, it is often referred to as the model for perfectly complementary resources by those using the resource classification of León and Tumpson. By (5), the resource growth isoclines (in the (R_1,R_2)-plane) also form corners. Thus, this is also called the model for essential resources by those using the classification of Tilman. (Note that Tilman used the classification "complementary resources" in a completely different sense, as a special case of his substitutable resources.)

In order to describe the zero net growth isoclines for resources fulfilling different growth needs, it will be convenient to establish the following notation for the break-even concentration for population i on resource R_j when the other resource is abundant and hence nonlimiting. Define R_{j_i} so that

$$p_{ij}(R_{j_i})=D. \tag{19}$$

By the monotonicity of $p_{ij}(R_j)$, R_{j_i} is a uniquely defined extended positive real number provided we assume that $R_{j_i}=\infty$ if $p_{ij}(R_j)<D$ for all $R_j\geq 0$. When both resources are supplied in growth-limiting amounts, we have $\mu_i(R_{1_i},R_2)=D$ for all $R_2\geq R_{2_i}$ and $\mu_i(R_1,R_{2_i})=D$ for all $R_1\geq R_{1_i}$, giving an L-shaped curve of break-even concentrations with corner at (R_{1_i},R_{2_i}) in the (R_1,R_2)-plane. More generally, for model (18), when two resources fulfill different needs (and hence neither can sustain the population independently) the zero net growth isocline need not form corners. However, it does not intersect the R_1 and R_2 axes, and runs parallel to them asymptotically. This will be in stark contrast to the resources considered in the next section

B.2 Resources that fulfill the same growth needs

We now consider resources such that each can sustain growth in the absence of the other, and hence the zero net growth isocline intersects both axes. Thus, there is a finite concentration R_{1_i} of resource R_1 with $\mu_i(R_{1_i},0)=D$

and a finite concentration R_{2_i} of resource R_2 with $\mu_i(0, R_{2_i}) = D$. In this case that resources fulfill the same growth needs, growth is often modeled (e.g. [3, 17, 22]) by a sum (as in (6)):

$$\mu_i(R_1, R_2) = Y_{i1}\mu_{i1}(R_1, R_2) + Y_{i2}\mu_{i2}(R_1, R_2),$$

where the constants Y_{ij} are growth yield constants. In this case, the indifference curves (in the (μ_{i1}, μ_{i2})-plane) are linear and so the resources are called perfectly substitutable according to the resource classification of León and Tumpson. On the other hand, such resources are only called perfectly substitutable in the classification of Tilman if the resource growth isoclines (obtained by further projecting $\mu_i(R_1, R_2) = C$ into the (R_1, R_2)-plane) are linear. This is the case when the familiar Michaelis-Menten or Monod functional response is generalized to the case of two perfectly substitutable resources (see [28]). That is, choosing

$$\mu_{i1}(R_1, R_2) = \frac{m_{i1}K_{i2}R_1}{K_{i1}K_{i2} + K_{i2}R_1 + K_{i1}R_2},\ \mu_{i2}(R_1, R_2) = \frac{m_{i2}K_{i1}R_2}{K_{i1}K_{i2} + K_{i2}R_1 + K_{i1}R_2}, \tag{20}$$

(as in (10)) yields both indifference curves and resource growth isoclines that are linear, and hence the two classifications are consistent. However, we need not deviate far from (20) to find an example for which this consistency fails to hold. Taking

$$\mu_{i1}(R_1, R_2) = \frac{m_{i1}R_1}{K_{i1} + R_1} \text{ and } \mu_{i2}(R_1, R_2) = \frac{m_{i2}R_2}{K_{i2} + R_2}$$

in (6) we obtain linear indifference curves, but resource growth isoclines that are convex, linear, or concave, depending on the values of the parameters, and hence classified as complementary, perfectly substitutable, or antagonistic, in the terminology of Tilman.

As one of the examples to illustrate our method, we assume (6) and (10) hold, since the resulting model can be referred to as perfectly substitutable in the classifications of both León and Tumpson and Tilman, and because the resulting model represents an extreme case compared to model (4). However, the method can be applied more generally. For example, when resources fulfill the same needs for growth and we impose (6), it might be reasonable to assume that the consumption of resource j by population i increases strictly with the availability of resource j, as in (8), but that it decreases with the availability of the other resource, as in (9) (see [3, 22]). The latter (9) incorporates the possibly inhibitory effect that the abundant presence of one resource might have on the consumption of the other due to handling time. In particular, the generalized Michaelis-Menten functions (20) satisfy these assumptions.

B.3 Resources that fall between the extremes

In reality, use of most resources fall somewhere in between the extremes discussed thus far, and the level curve of break-even concentrations might intersect one axis and not the other. The graphical method we present can

be applied very generally to locate single-species and coexistence equilibria and determine their stability. In fact, only the basic assumptions given in Section 1.2 for model (2) are necessary to locate the equilibria. Additional assumptions are needed only to determine their stability, though these condition are not restrictive. Besides the special cases discussed in the previous subsections, stability can be determined for model (2) without requiring (6) provided we assume (7), (8), and

$$|\frac{\partial \mu_{i1}}{\partial R_2}(R_1, R_2)|, \quad |\frac{\partial \mu_{i2}}{\partial R_1}(R_1, R_2)| \text{ are relatively small } \quad i = 1,\ 2, \tag{21}$$

so that the external concentration of one resource has a relatively small effect on the consumption of the other. This allows for more complicated resources that might fully or partially fulfill the same requirement for growth, and/or might have a synergistic or inhibitory effect if taken together. Perhaps such an assumption is not unreasonable; indeed, León and Tumpson [17] only consider the case when there is no such effect, i.e.

$$\frac{\partial \mu_{i1}}{\partial R_2}(R_1, R_2) = \frac{\partial \mu_{i2}}{\partial R_1}(R_1, R_2) = 0.$$

Details concerning the stability are provided in Section 2 and Appendix D. Note that the method also works when the resources are inhibitory at high concentrations, in which case the level curve of break-even concentrations could be a closed curve.

C Generalizations

Step 6 in Section 2 was stated under the assumption that ZNGI_i intersects both FSB_j and ZNGI_j at most once, $i, j \in \{1, 2\}$ and that any such intersection is transversal. We also assumed the resulting single species equilibrium to be globally asymptotically stable with respect to the (R_1, R_2, N_i)-subsystem. Here we examine the implications of generalizing these assumptions.

C.1 Multiple crossings of ZNGI_i and FSB_j

First we consider the nature of the feasible set boundaries in (R_1, R_2)-space. From (11), FSB_j is given by

$$\mu_{j2}(R_1, R_2)(S_1 - R_1) = \mu_{j1}(R_1, R_2)(S_2 - R_2). \tag{22}$$

In the case of model (4), FSB_j is a line with slope $Y_{j1}/Y_{j2} > 0$ (see (12)). Otherwise, consider R_2 in (22) to be a function of R_1. Differentiating with respect to R_1 we have

$$\begin{aligned} &\frac{\partial R_2}{\partial R_1}\left(\frac{\partial \mu_{j2}}{\partial R_2}(S_1 - R_1) + \mu_{j1} - \frac{\partial \mu_{j1}}{\partial R_2}(S_2 - R_2)\right) \\ &= \mu_{j2} - \frac{\partial \mu_{j2}}{\partial R_1}(S_1 - R_1) + \frac{\partial \mu_{j1}}{\partial R_1}(S_2 - R_2). \end{aligned}$$

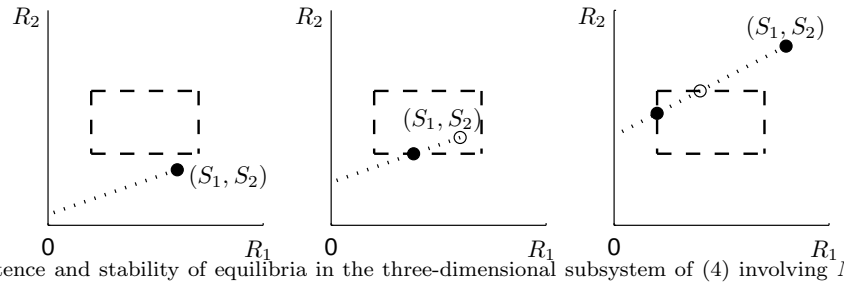

Fig. 8 The existence and stability of equilibria in the three-dimensional subsystem of (4) involving N_1 (in the absence of N_2) is depicted when resources are inhibitory at high concentrations. The dashed rectangle denotes ZNGI_1 with interior $\mathcal{R}_1$, while the dotted line depicts FSB_2.

Under assumptions ((8) and (9)) or ((8) and (21)), it follows that $\partial R_2/\partial R_1 > 0$. If ZNGI_i is decreasing, it can intersect FSB_j at most once.

For an example in which ZNGI_i and FSB_j intersect more than once, we turn to the case of inhibition in the context of essential resources, i.e. the resources are limiting at both low and high concentrations. (See [7].) Here we remove the assumption on the derivative of p_{ij} and assume that each equation $p_{ij}(R_j) = D$ has precisely two solutions. Denote these solutions by $R_{j_i}^1 < R_{j_i}^2$, and note that $p'_{ij}(R_{j_i}^1) > 0$ while $p'_{ij}(R_{j_i}^2) < 0$. That there are two such solutions will impact neither the FSBs nor $\mathcal{F}$, but ZNGI_i now forms a rectangle in the (R_1, R_2)-plane. Denote by $\mathcal{R}_i$ the interior of this rectangle. Note that ZNGI_i intersects FSB_j at most two times.

As depicted in Figure 8, we first consider a single species N_1 growing on the two resources (i.e. $N_2 = 0$). (Of course, the choice of subscripts is completely arbitrary.) We consider the stability of this three-dimensional subsystem of (4). If the supply point is in $\mathcal{R}_1$, then the washout equilibrium is unstable; if it is not in the closure of $\mathcal{R}_1$, then it is locally asymptotically stable. Recall that FSB_2 is determined by $R_1' = 0 = R_2'$ with $N_2 = 0$, i.e. in the absence of species N_2. Single-species equilibria correspond to intersections of ZNGI_1 and FSB_2. These equilibria alternate in stability as one moves from the supply point to a coordinate axis. This follows from a standard local stability computation involving the eigenvalues of the three-dimensional Jacobian evaluated at the single-species equilibrium. One of the eigenvalues has the opposite sign to $p'_{1j}(R_{j_1}^k)$, while the remaining two are both equal to $-D$.

Now suppose that competitor N_2 is introduced, and consider how this affects the stability of the equilibria just discussed as they occur in the full four-dimensional system. If the supply point is in $\mathcal{R}_1 \cup \mathcal{R}_2$, then the washout equilibrium is unstable. If it is not in the closure of $\mathcal{R}_1 \cup \mathcal{R}_2$, then it is locally asymptotically stable. A standard linear analysis of the full four-dimensional system at an equilibrium of the form $E_1 = (\bar{R}_{1_1}, \bar{R}_{2_1}, \bar{N}_1, 0)$ reveals that three of the eigenvalues remain as in the previous paragraph. The fourth eigenvalue is given by $\mathcal{G}_2(\bar{R}_{1_1}, \bar{R}_{2_1}) - D$,

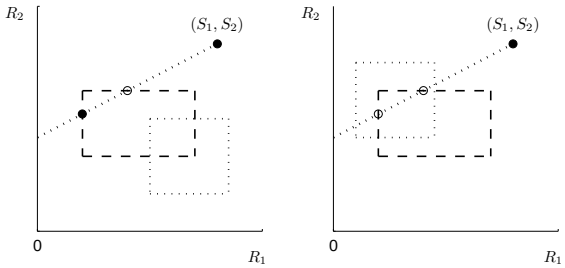

Fig. 9 How the inclusion of ZNGI_2 for competitor N_2 affects the stability of the single-species equilibria involving N_1 in Figure 8(RIGHT).

and hence its sign is determined by the invasion criterion. It follows that E_1 remains unstable with the addition of competitor N_2 if it was unstable in the (R_1, R_2, N_1)-subsystem. Further, suppose E_1 was locally asymptotically stable in the (R_1, R_2, N_1)-subsystem. If $(\bar{R}_{1_1}, \bar{R}_{2_1})$ is not in the closure of $\mathcal{R}_2$, then E_1 remains asymptotically stable (see Figure 9(LEFT)). However, if $(\bar{R}_{1_1}, \bar{R}_{2_1})$ is in $\mathcal{R}_2$, then E_1 is unstable (see Figure 9(RIGHT)).

Finally, any intersection of the ZNGIs in $\mathcal{F}$ that is not on the boundary of $\mathcal{F}$ corresponds to a coexistence equilibrium. The issue of the stability of such an equilibrium is complicated, since this system can exhibit nontrivial dynamics. See Butler and Wolkowicz [7] for a more detailed discussion. For example, it is shown that a coexistence equilibrium can undergo a Hopf bifurcation.

C.2 Multiple intersections of the ZNGI

Now consider the stability of equilibria when there are multiple crossings of the ZNGIs, as in Figure 9A of [24]. We will require the following notation:

- The supply point (S_1, S_2) corresponds to the washout equilibrium $E_0 = (S_1, S_2, 0, 0)$.
- If ZNGI_1 intersects FSB_2, denote the point of intersection by $(\bar{R}_{1_1}, \bar{R}_{2_1})$. This corresponds to a single-species equilibrium of the form $E_1 = (\bar{R}_{1_1}, \bar{R}_{2_1}, \bar{N}_1, 0)$ with $\bar{N}_1 > 0$. Similarly, if ZNGI_2 intersects FSB_1, denote the point of intersection by $(\bar{R}_{1_2}, \bar{R}_{2_2})$. This corresponds to a single-species equilibrium of the form $E_2 = (\bar{R}_{1_2}, \bar{R}_{2_2}, 0, \bar{N}_2)$ with $\bar{N}_2 > 0$.
- Identify coexistence equilibria, denoted $E^* = (R_1^*, R_2^*, N_1^*, N_2^*)$ with $N_i^* > 0$, $i = 1, 2$, as points where ZNGI_1 and ZNGI_2 intersect in the interior of $\mathcal{F}$.

Theorem 3.14 of [3] holds for any monotone decreasing ZNGI under assumptions ((8) and (9)) or ((8) and (21)). In particular, for any intersection (R_1^*, R_2^*) of the ZNGIs, we have

$$\min\{\bar{R}_{1_1}, \bar{R}_{1_2}\} < R_1^* < \max\{\bar{R}_{1_1}, \bar{R}_{1_2}\},$$

and the determinant (16) maintains its sign on the interval

$$(\min\{\bar{R}_{1_1}, \bar{R}_{1_2}\}, \max\{\bar{R}_{1_1}, \bar{R}_{1_2}\}).$$

As one moves from the single-species equilibrium along the corresponding ZNGI, only the inequality $|\varphi_1'(R_1^*)| > |\varphi_2'(R_1^*)|$ reverses with each transversal crossing of the ZNGIs. Thus, $A_4 > 0$ and $A_4 < 0$ (in turn) at each crossing. (See Appendix D.2.)

C.3 Assumptions for Step 6 in Section 2 hold more generally

Step 6 in Section 2 was stated under the assumption that any single-species equilibrium is globally asymptotically stable with respect to the (R_1, R_2, N_i)-subsystem. Indeed, this is the case for system (4) (see [7]) and for system (2) with $g_j(R_j) = (S_j - R_j)D$ and $D_i = D$ assuming (6), (7), (8), and (9) (see [3]). A standard linear analysis of the (R_1, R_2, N_i)-subsystems of (2) (based in the chemostat) indicates that local asymptotic stability of such an equilibrium does not require (6) and (9), under assumptions (7) and (8) provided (21) holds. (See [21] and Appendix D.1).

D Local Stability

D.1 Stability of a single species equilibrium

Determining the local asymptotic stability of an interior equilibrium from the corresponding variational matrix is necessarily computational. For the (R_1, R_2, N_i)-subsystem, necessary and sufficient conditions have been established both for perfectly substitutable resources (model (2) with assumptions (6), (7), (8), and (9) see [3]) and for essential resources (model (4) with assumptions (5), see [7]). In this appendix we give the details of a standard linear analysis of the (R_1, R_2, N_i)-subsystems of (2). Consider

$$\begin{aligned} R_j' &= (S_j - R_j)D - N_i\mu_{ij}(R_1, R_2), \\ N_i' &= N_i(-D + \mu_i(R_1, R_2)). \end{aligned}$$

Let us assume that a one-species survival equilibrium $E_i = (\bar{R}_{1_i}, \bar{R}_{2_i}, \bar{N}_i)$ exists, and examine the local stability properties of E_i. The variational matrix evaluated at E_i is given by

$$\begin{pmatrix} -D - \frac{\bar{N}_i}{Y_{i1}}\frac{\partial \mu_{i1}}{\partial R_1} & -\frac{\bar{N}_i}{Y_{i1}}\frac{\partial \mu_{i1}}{\partial R_2} & -\frac{1}{Y_{i1}}\mu_{i1} \\ -\frac{\bar{N}_i}{Y_{i2}}\frac{\partial \mu_{i2}}{\partial R_1} & -D - \frac{\bar{N}_i}{Y_{i2}}\frac{\partial \mu_{i2}}{\partial R_2} & -\frac{1}{Y_{i2}}\mu_{i2} \\ \bar{N}_i\frac{\partial \mu_i}{\partial R_1} & \bar{N}_i\frac{\partial \mu_i}{\partial R_2} & 0 \end{pmatrix}.$$

The characteristic equation of $V(\bar{R}_{1_i}, \bar{R}_{2_i}, \bar{N}_i)$, the variational matrix evaluated at E_i, is given by $\lambda^3 + A_1\lambda^2 + A_2\lambda + A_3$, where

$$\begin{aligned} A_1 &= 2D + \frac{\bar{N}_i}{Y_{i1}}\frac{\partial \mu_{i1}}{\partial R_1} + \frac{\bar{N}_i}{Y_{i2}}\frac{\partial \mu_{i2}}{\partial R_2}, \\ A_2 &= D^2 + \frac{\bar{N}_i^2}{Y_{i1}Y_{i2}}\left(\frac{\partial \mu_{i1}}{\partial R_1}\frac{\partial \mu_{i2}}{\partial R_2} - \frac{\partial \mu_{i2}}{\partial R_1}\frac{\partial \mu_{i1}}{\partial R_2}\right) \\ &\quad + \bar{N}_i\left(\frac{\mu_{i2}}{Y_{i2}}\frac{\partial \mu_i}{\partial R_2} + \frac{\mu_{i1}}{Y_{i1}}\frac{\partial \mu_i}{\partial R_1} + \frac{D}{Y_{i1}}\frac{\partial \mu_{i1}}{\partial R_1} + \frac{D}{Y_{i2}}\frac{\partial \mu_{i2}}{\partial R_2}\right), \\ A_3 &= \bar{N}_i D\left(\frac{\mu_{i1}}{Y_{i1}}\frac{\partial \mu_i}{\partial R_1} + \frac{\mu_{i2}}{Y_{i2}}\frac{\partial \mu_i}{\partial R_2}\right) \\ &\quad + \frac{\bar{N}_i^2}{Y_{i1}Y_{i2}}\left(\frac{\partial \mu_i}{\partial R_2}\left(\mu_{i2}\frac{\partial \mu_{i1}}{\partial R_1} - \mu_{i1}\frac{\partial \mu_{i2}}{\partial R_1}\right) + \frac{\partial \mu_i}{\partial R_1}\left(\mu_{i1}\frac{\partial \mu_{i2}}{\partial R_2} - \mu_{i2}\frac{\partial \mu_{i1}}{\partial R_2}\right)\right), \end{aligned}$$

and $A_1A_2 - A_3 = B_1\bar{N}_i^3 + B_2\bar{N}_i^2 + B_3\bar{N}_i + B_4$, where

$$\begin{aligned} B_4 &= 2D^3, \\ B_3 &= 3D^2\left(\frac{1}{Y_{i1}}\frac{\partial \mu_{i1}}{\partial R_1} + \frac{1}{Y_{i2}}\frac{\partial \mu_{i2}}{\partial R_2}\right) + D\left(\frac{\mu_{i1}}{Y_{i1}}\frac{\partial \mu_i}{\partial R_1} + \frac{\mu_{i2}}{Y_{i2}}\frac{\partial \mu_i}{\partial R_2}\right) \\ B_2 &= D\left(\frac{1}{Y_{i1}}\frac{\partial \mu_{i1}}{\partial R_1} + \frac{1}{Y_{i2}}\frac{\partial \mu_{i2}}{\partial R_2}\right)^2 + \frac{2D}{Y_{i1}Y_{i2}}\left(\frac{\partial \mu_{i1}}{\partial R_1}\frac{\partial \mu_{i2}}{\partial R_2} - \frac{\partial \mu_{i2}}{\partial R_1}\frac{\partial \mu_{i1}}{\partial R_2}\right) \\ &\quad + \frac{1}{Y_{i1}^2}\frac{\partial \mu_i}{\partial R_1}\frac{\partial \mu_{i1}}{\partial R_1}\mu_{i1} + \frac{1}{Y_{i1}Y_{i2}}\left(\frac{\partial \mu_i}{\partial R_1}\frac{\partial \mu_{i1}}{\partial R_2}\mu_{i2} + \frac{\partial \mu_i}{\partial R_2}\frac{\partial \mu_{i2}}{\partial R_1}\mu_{i1}\right) + \frac{1}{Y_{i2}^2}\frac{\partial \mu_i}{\partial R_2}\frac{\partial \mu_{i2}}{\partial R_2}\mu_{i2} \\ B_1 &= \frac{1}{Y_{i1}Y_{i2}}\left(\frac{\partial \mu_{i1}}{\partial R_1}\frac{\partial \mu_{i2}}{\partial R_2} - \frac{\partial \mu_{i2}}{\partial R_1}\frac{\partial \mu_{i1}}{\partial R_2}\right)\left(\frac{1}{Y_{i1}}\frac{\partial \mu_{i1}}{\partial R_1} + \frac{1}{Y_{i2}}\frac{\partial \mu_{i2}}{\partial R_2}\right). \end{aligned}$$

An examination of the A_i and B_i indicates that such an equilibrium is locally asymptotically stable whenever (7), (8), and (21) hold.

D.2 Stability of a unique coexistence equilibrium

We examine the details of the stability of a coexistence equilibrium at a unique intersection of the ZNGI. Determining the local asymptotic stability of an interior equilibrium from the corresponding variational matrix is

necessarily computational. Necessary and sufficient conditions have been established for model (4) with assumptions (5) (see [7]), and necessary conditions have been established by various authors for special cases of model (2) [3, 17]. In this section, we examine this same question in the context of the most general model (2). Denote by $\lambda^4 + A_1\lambda^3 + A_2\lambda^2 + A_3\lambda + A_4$ the characteristic polynomial of the variational matrix of (2) evaluated at a coexistence equilibrium $E^* = (R_1^*, R_2^*, N_1^*, N_2^*)$. Then a necessary condition for E^* to be locally asymptotically stable is

$$A_4 = \left(\frac{\partial \mu_1}{\partial R_1}\frac{\partial \mu_2}{\partial R_2} - \frac{\partial \mu_1}{\partial R_2}\frac{\partial \mu_2}{\partial R_1}\right)(\mu_{11}\mu_{22} - \mu_{12}\mu_{21}) > 0, \tag{23}$$

where each of these quantities is evaluated at the interior equilibrium (if it exists). Suppose the ZNGIs intersect transversally at (R_1^*, R_2^*) inside the feasible set. Without loss of generality, assume that $\bar{R}_{1_1} < \bar{R}_{1_2}$, as it is in Figure 5. We will examine each factor of A_4 in turn.

Consider the first multiplicative factor of A_4. Suppose that $\mu_i(R_1, R_2)$ is increasing in both variables. As in Lemma 3.5 of [3], one can show that there exists a C^1 function $\varphi_i(R_1)$ (corresponding to ZNGI_i) satisfying $\mu_i(R_1, \varphi_i(R_1)) = D$ with

$$\varphi_i'(R_1) = -\frac{(\partial/\partial R_1)\mu_i(R_1, \varphi_i(R_1))}{(\partial/\partial R_2)\mu_i(R_1, \varphi_i(R_1))} < 0.$$

If the single-species equilibria are locally asymptotically stable (as in Figure 5(BOTTOM,MIDDLE)), then $(\bar{R}_{1_1}, \bar{R}_{2_1})$ is in the complement of $\mathcal{I}_2$ while $(\bar{R}_{1_2}, \bar{R}_{2_2})$ is in the complement of $\mathcal{I}_1$. This implies $|\varphi_1'(R_1^*)| < |\varphi_2'(R_1^*)|$, so that

$$\frac{\partial \mu_1}{\partial R_1}\frac{\partial \mu_2}{\partial R_2} - \frac{\partial \mu_1}{\partial R_2}\frac{\partial \mu_2}{\partial R_1} < 0.$$

If the single-species equilibria are unstable (as in Figure 5(BOTTOM,RIGHT)), then $(\bar{R}_{1_1}, \bar{R}_{2_1})$ is in $\mathcal{I}_2$ while $(\bar{R}_{1_2}, \bar{R}_{2_2})$ is in $\mathcal{I}_1$. This implies $|\varphi_1'(R_1^*)| > |\varphi_2'(R_1^*)|$, so that

$$\frac{\partial \mu_1}{\partial R_1}\frac{\partial \mu_2}{\partial R_2} - \frac{\partial \mu_1}{\partial R_2}\frac{\partial \mu_2}{\partial R_1} > 0.$$

We now examine the second multiplicative factor of A_4. At the intersection of the ZNGIs, the equations $R_1' = 0 = R_2'$ yield N_1^* and N_2^* as in (15) with $\Delta(R_1^*, R_2^*)$ as in (16). Note that $\Delta(R_1^*, R_2^*)$ is indeed the second factor. The techniques of Lemma 3.13 and Theorem 3.14 of [3] can be applied under assumptions ((8) and (9)) or ((8) and (21)) to show that $\Delta(R_1^*, R_2^*) > 0$ (since $\bar{R}_{1_1} < \bar{R}_{1_2}$, as in Figure 5). In particular, consider the numerator of N_i^* in (15) to be a function of R_1 by restricting R_2 to $\varphi_j(R_1)$, and denote the result by $\mathcal{N}_i(R_1)$. It can be shown that $\mathcal{N}_i(\bar{R}_{1_j}) = 0$, $\mathcal{N}_1(R_1)$ is decreasing on $(\bar{R}_{1_1}, \bar{R}_{1_2})$, and $\mathcal{N}_2(R_1)$ is increasing on $(\bar{R}_{1_1}, \bar{R}_{1_2})$. Thus, each is positive, and so $\Delta(R_1^*, R_2^*) > 0$. Therefore, if the single-species equilibria are locally asymptotically stable, $A_4 < 0$ (and so E^* is unstable). However, if the single-species equilibria are unstable, then $A_4 > 0$. (Note that $\Delta(R_1^*, R_2^*) < 0$ when $\bar{R}_{1_1} > \bar{R}_{1_2}$.)

For model (4), consider the configuration in Figure 5(TOP,MIDDLE). At E^* species one is limited by resource two (so that $\mu_1(R_1^*, R_2^*) = p_{12}(R_2^*)$) and species two is limited by resource one (so that $\mu_2(R_1^*, R_2^*) = p_{21}(R_1^*)$). Therefore, at (R_1^*, R_2^*),

$$\frac{\partial \mu_1}{\partial R_1}\frac{\partial \mu_2}{\partial R_2} - \frac{\partial \mu_1}{\partial R_2}\frac{\partial \mu_2}{\partial R_1} = -p_{12}' \cdot p_{21}' < 0.$$

At $\bar{E}_1$, $\mu_{11}(R_1, R_2) = p_{11}(R_1)/Y_{11}$, $\mu_{12}(R_1, R_2) = p_{11}(R_1)/Y_{12}$, and $\bar{N}_2 = 0$. Along the vertical portion of ZNGI_1, the numerator of N_2^* in (15) is given by

$$(S_2 - R_2)p_{11}(R_1)/Y_{11} - (S_1 - R_1)p_{11}(R_1)/Y_{12}.$$

This is a decreasing function of R_2, so as R_2 decreases from $\bar{R}_{2_1}$ to R_{2_1}, this expression increases from zero. At (R_{1_1}, R_{2_1}) species one becomes limited by resource two, so that $\mu_{11}(R_1, R_2) = p_{12}(R_2)/Y_{11}$, $\mu_{12}(R_1, R_2) = p_{12}(R_2)/Y_{12}$, and the numerator of N_2^* in (15) is given by

$$(S_2 - R_2)p_{12}(R_2)/Y_{11} - (S_1 - R_1)p_{12}(R_2)/Y_{12}.$$

This is an increasing function of R_1, so as R_1 increases from R_{1_1} to R_1^*, this expression increases still more. Thus, the numerator of N_2^* in (15) is positive at E^*. Similarly, one can show that the numerator of N_1^* in (15) is positive at E^*. This gives $\Delta(R_1^*, R_2^*) > 0$, implying that $A_4 < 0$ and the coexistence equilibrium is unstable. Note that other configurations are possible in Figure 5(TOP,MIDDLE) (by moving one or both of the FSBs), but the argument will proceed as above.

For the configuration in Figure 5(TOP,RIGHT), species one is limited by resource one (so that $\mu_1(R_1^*, R_2^*) = p_{11}(R_1^*)$) and species two is limited by resource two (so that $\mu_2(R_1^*, R_2^*) = p_{22}(R_2^*)$). Therefore, at (R_1^*, R_2^*),

$$\frac{\partial \mu_1}{\partial R_1}\frac{\partial \mu_2}{\partial R_2} - \frac{\partial \mu_1}{\partial R_2}\frac{\partial \mu_2}{\partial R_1} = p_{11}' \cdot p_{22}' > 0.$$

As in the previous paragraph, one can determine that the numerators of both N_1^* and N_2^* in (15) are positive at E^*, giving $\Delta(R_1^*, R_2^*) > 0$, so that $A_4 > 0$. It is interesting to note that in the case of Figure 5(TOP,RIGHT), where the coexistence equilibrium is stable, each species must be limited by the same resource at the coexistence equilibrium that it would be limited by at the single-species equilibrium.

For essential resources, the interpretation of the sign of this first component is the same as in the previous case but can be more simply stated: each species is limited by a different resource. The second component of A_4 now yields the following necessary condition for stability: the product of the consumption rates of the nutrient that is limiting (essential) or more limiting (substitutable) for each species is larger than the product of the consumption rates of the non-limiting (essential) or less limiting (substitutable) nutrient for each species.

Acknowledgements Research of GSKW partially supported by the Natural Science and Engineering Research Council of Canada.

We would like to thank "The Lunch Bunch" at Cornell: Stephen Ellner, Laura Jones, Paul Hurtado, Michael Cortez, and Kathryn Sullivan, for their encouragement and for providing invaluable suggestions after reading an earlier version.

We would also like to thank the referees whose suggestions improved the clarity of the manuscript.

References

1. Bader F (1978) Analysis of double-substrate limited growth. Biotechnol Bioeng 20:183–202
2. Bader F, Meyer J, Fredrickson A, Tsuchiya H (1975) Comments on microbial growth rate. Biotechnol Bioeng 17:279–283
3. Ballyk MM, Wolkowicz GSK (1993) Exploitative competition in the chemostat on two perfectly substitutable resources. Math Biosci 118:127–180
4. Ballyk MM, Wolkowicz GSK (1995) An examination of the thresholds of enrichment: A resource-based growth model. J Math Biol 33:435–457
5. Ballyk MM, McCluskey CC, Wolkowicz GSK (2005) Global analysis of competition for perfectly substitutable resources with linear response. J Math Biol 51:458–490
6. Butler GJ, Wolkowicz GSK (1985) A mathematical model of the chemostat with a general class of functions describing nutrient uptake. SIAM J Appl Math 45(1):138–151
7. Butler GJ, Wolkowicz GSK (1987) Exploitative competition in the chemostat for two complementary, and possibly inhibitory, resource. Math Biosci 83:1–48
8. Egli T (1995) The ecological and physiological significance of the growth of heterotrophic microorganisms with mixtures of substrates. Adv Microb Ecol 14:305–386
9. Freedman HI, Waltman P (1984) Persistence in models of three interacting predator-prey populations. Math Biosci 68:213–231
10. Gause GF (1934) The struggle for existence. Williams and Wilkins, Baltimore, MD

11. Grover JP (1997) Resource competition. Population and community biology series 19. Chapman and Hall, New York

12. Harder W, Dijkhuizen L (1976) Mixed substrate utilization in microorganisms. In: Continuous culture, (Applications and newfields) (ed. A. C. R. Dean, D. C. Ellwood, C. G. T. Evans and J. Melling), vol 6, Ellis Horwood, Chichester and Oxford, pp 297–314

13. Hsu SB (1978) Limiting behavior for competing species. SIAM J Appl Math 34:760–763

14. Hsu SB, Hubbell SP, Waltman P (1977) A mathematical theory of single nutrient competition in continuous cultures for microorganisms. SIAM J Appl Math 32:366–383

15. Hsu SB, Cheng KS, Hubbell SP (1981) Exploitative competition of microorganisms for two complementary nutrients in continuous culture. SIAM J Appl Math 41:422–444

16. Huisman J, Weissing FJ (1999) Biodiversity of plankton by species oscillations and chaos. Nature 402:407–410

17. León JA, Tumpson DB (1975) Competition between two species for two complementary or substitutable resources. J Theor Biol 50:185–2012

18. Li B (1999) Global asymptotic behavior of the chemostat: general response functions and differential death rates. SIAM J Appl Math 59:411–422

19. Li B, Smith HL (2001) How many species can two essential resources support? SIAM J Appl Math 62:336–366

20. Lotka AJ (1925) Elements of Physical Biology. Williams and Wilkins, Baltimore

21. Phillips O (1973) The equilibrium and stability of simple marine biological systems i. primary nutrient consumers. Am Nat 107:73–93

22. Pilyugin SS, Reeves GT, Narang A (2004) Predicting stability of mixed microbial cultures from single species experiments: 1. phenomenological model. Math Biosci 192:85–105

23. Rapport DJ (1971) An optimization model of food selections. Am Nat 105:575–587

24. Tilman D (1980) Resources: A graphical-mechanistic approach to competition and predation. Am Nat 116:362–393

25. Tilman D (1982) Resource competition and community structure. Princeton University Press, New Jersey

26. Verhulst PF (1838) Notice sur la loi que la population suit dans son accroissement. Correspondance Mathematique et Physique 10:113–121

27. Volterra V (1928) Variations and fluctuations of the number of individuals in animal species living together. J Conserv (Conserv Int Explor Mer) 3:3–51

28. Waltman P, Hubbell SP, Hsu SB (1980) Theoretical and experimental investigations of microbial competition in continuous culture. In: Burton T (ed) Modeling and Differential Equations, Marcel Dekker, New York, pp 107–152

29. Wolkowicz GSK, Lu Z (1992) Global dynamics of a mathematical model of competition in the chemostat: general response functions and differential death rates. SIAM J Appl Math 52(1):222–233

30. Wolkowicz GSK, Xia H (1997) Global asymptotic behavior of a chemostat model with discrete delays. SIAM J Appl Math 57(4):1019–1043

31. Wolkowicz GSK, Xia H, Ruan S (1997) Competition in the chemostat: A distributed delay model and its global asymptotic behavior. SIAM J Appl Math 57(5):1281–1310

32. Wolkowicz GSK, Xia H, Wu J (1999) Global dynamics of a chemostat competition model with distributed delay. J Math Biol 38:285–316